HETEROCYCLES, Vol. 102, No. 10, 2021, pp. 1939 - 1947. © 2021 The Japan Institute of Heterocyclic Chemistry
Received, 8th June, 2021, Accepted, 7th July, 2021, Published online, 27th July, 2021
DOI: 10.3987/COM-21-14502

# A LONG-WAVELENGTH EMISSION FLUORESCENT PROBE BASED ON TCF DERIVATIVES FOR HIGH-SENSITIVITY DETECTION OF $Hg^{2+}$

**Yuan Sun,[a] Keli Zhong,[a] Lijun Tang,[a,c]* and Xiaomei Yan[b]***

[a] College of Chemistry and Materials Engineering, Bohai University, Jinzhou 121013, China. E-mail: ljtang@bhu.edu.cn (L. Tang)

[b] College of Laboratory Medicine, Dalian Medical University, Dalian, 116044, China. E-mail: xmyan1978@sina.com (X. Yan)

[c] Department of Chemistry, National Demonstration Centre for Experimental Chemistry Education, Yanbian University, Yanji 133002, China.

**Abstract** – A new fluorescent probe **1** that derived from 2-dicyanomethylene-3-cyano-4,5,5-trimethyl-2,5-dihydrofuran (TCF) has been developed. Probe **1** displays selective recognition toward $Hg^{2+}$ in MeOH/Tris (1:1, v/v, Tris 20 mM, pH = 7.4) solution through fluorescence turn on behavior. The $Hg^{2+}$ sensing mechanism underwent $Hg^{2+}$-triggered removal of thiocarbonyl moiety of probe **1**, which resulting in releasing of the highly emissive compound **2**. The $Hg^{2+}$ recognition process holds some advantages including rapid response (<3 min), low detection limit (1.06 nM), and a large Stokes shift (160 nm). Cell imaging studies showed that probe **1** has membrane permeability and low toxicity to cells, and can be used to detect $Hg^{2+}$ in living cells.

Mercury is a highly toxic non-biological element that naturally exists in the environment.[1,2] At present, mercury is mainly used in the synthesis of chemicals and the manufacture of electronic or electrical products,[3] lead to the emission of mercury-containing pollutants.[4] Even at ppm levels of mercury accumulation,[5] it will also cause serious harm to the human brain,[6,7] heart, lung, kidney,[8] central nervous system and immune system.[9,10] Therefore, the highly sensitive and specific detection of mercury ion ($Hg^{2+}$) is of great significance to the environment and human health.[11,12]

The conventional methods for measuring $Hg^{2+}$ include atomic absorption spectrometry,[13,14] high performance liquid chromatography, electrochemical methods, and so on.[15,16] Although these methods are highly selective, they are time-consuming and labor-intensive, and usually require expensive equipment, making them difficult to detect $Hg^{2+}$ in real time.[17,18] Compared with the aforementioned methods,

fluorescence technology has attracted much attention due to its simple operation, fast response speed, high selectivity and sensitivity.[19,20] Therefore, a large number of researchers have developed small molecule fluorescent probes for the detection of mercury ions.[21,22] So far, many fluorescent probes based on formation of $Hg^{2+}$-ligand complex or $Hg^{2+}$-triggered reactions have been developed.[23] Among these methods, fluorescent probes based on ligand complexation usually show low selectivity.[24,25] Due to interference from other metal ions, the reaction-based $Hg^{2+}$ fluorescent probes have attracted considerable attention due to the high selectivity, simplicity, and unique spectra changes.[26,27] Due to the highly thiophilic nature of $Hg^{2+}$, the reaction type probes that have been developed mainly include the ring-opening of the spironolactone, $Hg^{2+}$ promoted cycloaddition of thiourea substrates, desulfurization of thioacetal substrates and thiocarbonyl,[28,29] etc. It is worth noting that only a few $Hg^{2+}$-specific fluorescent probes exhibit both long-wavelength emission and a large Stokes shift.[30,31] Therefore, it is still attractive to develop $Hg^{2+}$-specific fluorescent probes with long-wavelength emission and a large Stokes shift.[32,33]

2-Dicyanomethylene-3-cyano-4,5,5-trimethyl-2,5-dihydrofuran (TCF) possesses strong electron withdrawing ability, it usually acts as electron acceptor in the D-π-A conjugate system,[34] thus it has been widely used to construct long-wavelength emission fluorescent probes. Based on this idea, we herein designed and synthesized a TCF-derivatized fluorescence probe **1** (Scheme 1). The hydroxy group in compound **2** acts as an electron donor, formed D-π-A conjugated structure with TCF, the thiocarbonate moiety acts as both a quenching group and a recognition group, it can react selectively toward $Hg^{2+}$, leading to removal of thiocarbonyl and releasing of compound **2**, thus realizing $Hg^{2+}$-triggered fluorescence turn on response through restoration of intramolecualr charge transfer (ICT).

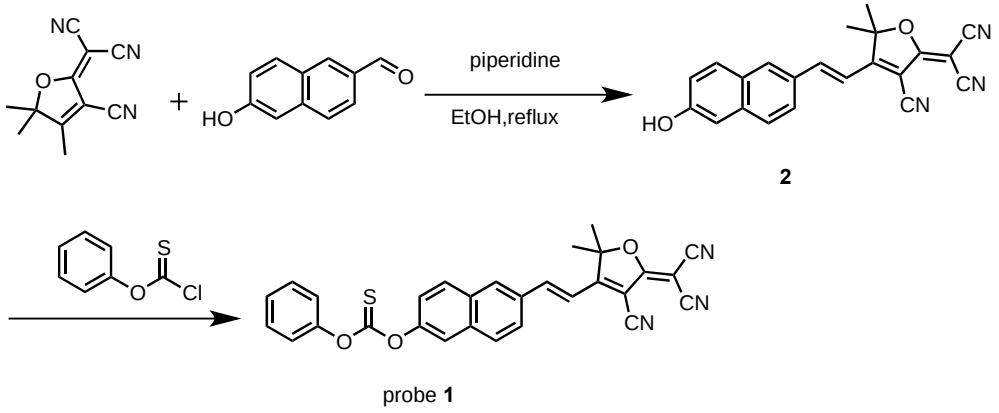


**Scheme 1.** Synthesis of the probe **1**

## Optical response of probe 1 to $Hg^{2+}$

We firstly studied the fluorescence response of probe **1** to different concentrations of $Hg^{2+}$ in MeOH/Tris (1:1, v/v, Tris 20 mM, pH = 7.4) solution. As shown in Figure 1, probe **1** solution shows weak fluorescence intensity at 550 nm, upon gradual addition of $Hg^{2+}$, a gradually increasing fluorescence

emission centered at 625 nm can be observed. When the added $Hg^{2+}$ reached 30 μM, the fluorescence intensity tends to be stable. This may due to the $Hg^{2+}$-triggered removal of the thiocarbonyl group, and the release of hydroxy group leading to enhanced ICT effects. These results prove that probe **1** has good sensing properties for $Hg^{2+}$. According to the titration curve, a satisfactory linear relationship is obtained between the fluorescence intensity ratios at 625 nm ($F/F_0$ relative intensity divided by the fluorescence intensity in the absence of metal ions) and the $Hg^{2+}$ (0-30 μM) concentration (Figure 2). The detection limit of probe **1** for $Hg^{2+}$ was then calculated to be 1.06 nM based on the equation LOD = $3\sigma/\rho$ ($\sigma$ is the standard deviation of the blank solution; $\rho$ is the slope of the calibration curve). At the same time, the time-dependent fluorescence intensity ratios ($F/F_0$) change of probe **1** to $Hg^{2+}$ (30 μM) was recorded, the response of probe **1** to $Hg^{2+}$ can be completed within 3 minutes (Figure 3), indicating that probe **1** is capable of detecting $Hg^{2+}$ in real time.

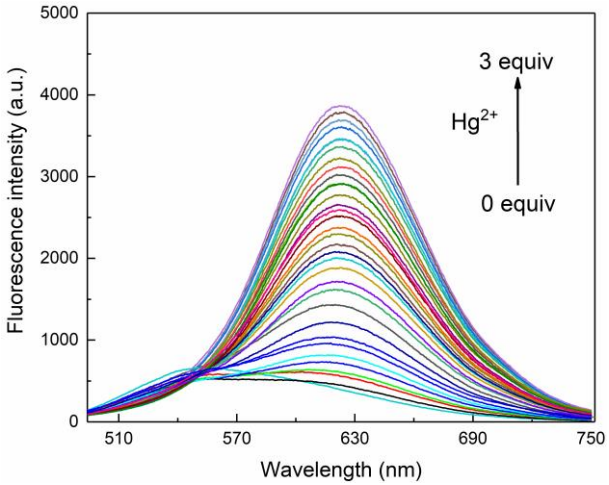


**Figure 1.** Changes of fluorescence spectra of probe **1** (10 μM) in MeOH/Tris (1:1, v/v, Tris 20 mM, pH = 7.4) solution with gradual addition of $Hg^{2+}$ (0-30 μM). $\lambda_{ex}$ = 465 nm

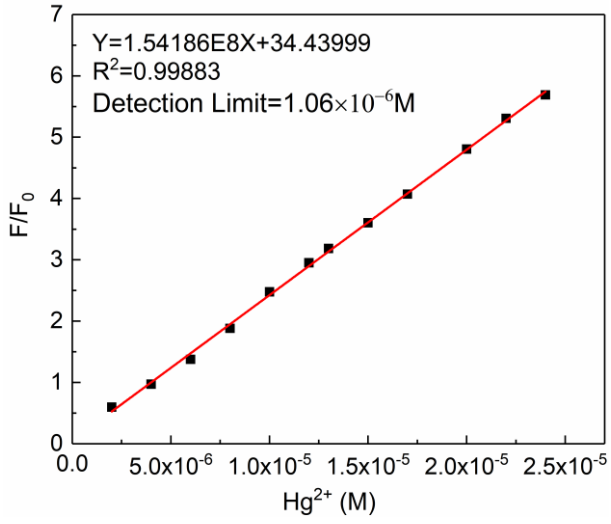


**Figure 2.** Linear relationship between fluorescence intensity ratios ($F/F_0$) and $Hg^{2+}$ concentration (0-30 μM)

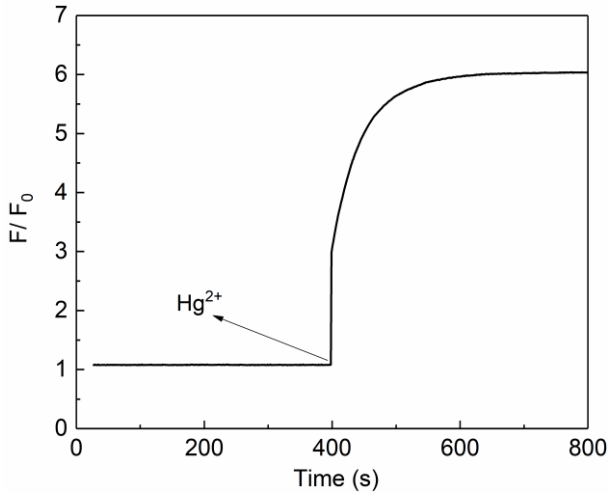


**Figure 3.** Time-dependent fluorescence intensity ratios ($F/F_0$) changes of probe **1** in the absence and presence of $Hg^{2+}$ (30 μM)

In order to verify the selectivity of probe **1** to $Hg^{2+}$, we detected the changes of the fluorescence spectra of probe **1** in the presence of different metal ions, including $Cu^{2+}$, $Co^{2+}$, $Zn^{2+}$, $Cd^{2+}$, $Cr^{3+}$, $Fe^{3+}$, $Sr^{2+}$, $Na^{+}$, $Hg^{2+}$, $Ag^{+}$ , $Pb^{2+}$, $Mn^{2+}$, $Al^{3+}$, $K^{+}$ , $Ni^{2+}$, $Ba^{2+}$, $Mg^{2+}$, $Fe^{2+}$ and $Ca^{2+}$ (3 equiv. of each) (Figure 4). It can be seen that the fluorescence intensity of probe **1** increased significantly at 625 nm on addition of $Hg^{2+}$ and $Ag^{+}$, however, no significant fluorescence enhancement was observed with the addition of other metal ions. Since $Ag^{+}$ and $Cl^{-}$ can readily form insoluble precipitate AgCl, the interference from $Ag^{+}$ can be effectively shielded by introducing an appropriate concentration of NaCl (Figure S1). We also compared the UV-vis absorption spectra of probe **1**, probe+$Ag^{+}$ and probe+$Hg^{2+}$ (Figure S2), the observed large overlap of the absorption spectra indicate that probe **1** is limited in detecting $Hg^{2+}$ by UV-vis absorption spectra. These results show that probe **1** has applicability for fluorescence detection of $Hg^{2+}$ in biological and environmental analysis.

To further validate the practicality of probe **1** for $Hg^{2+}$ detection, competition experiments were performed (Figure 5). In the presence of tested metal ions (except $Ag^{+}$), the fluorescence intensity of probe **1** remained almost unchanged. When $Hg^{2+}$ (30 μM) was subsequently added, the fluorescence intensity ratios ($F/F_0$) increased significantly at 625 nm. These results demonstrate that other coexisting metal ions (except for $Ag^{+}$) exert no obvious interference on $Hg^{2+}$ recognition. We also examined the effects of pH on $Hg^{2+}$ recognition by probe **1** (Figure 6). The fluorescence intensity ratios ($F/F_0$) of probe **1**+ $Hg^{2+}$ (3 equiv.) increased significantly between pH 5.0 and 9.0. The results show that probe **1** can detect $Hg^{2+}$ in a wide pH range, especially at near-neutral conditions.

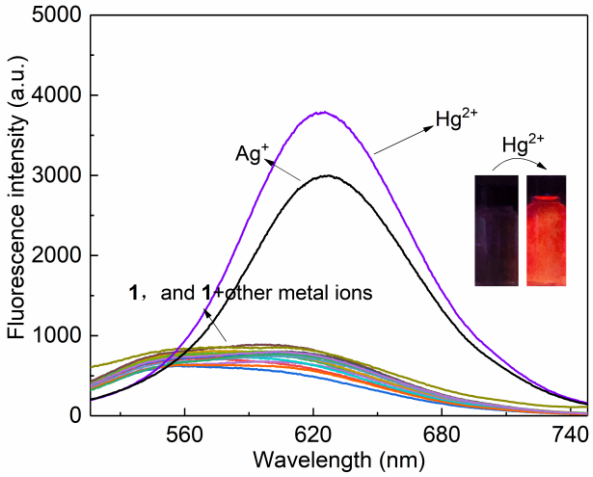


**Figure 4.** Fluorescence spectra changes of probe **1** (10 μM) in the presence of various a metal ions (30 μM) in MeOH/Tris (1:1, v/v, Tris 20 mM, pH = 7.4) solution. $\lambda_{ex}$ = 465 nm. Inset: Fluorescence photographs of the probe solution before and after adding $Hg^{2+}$.

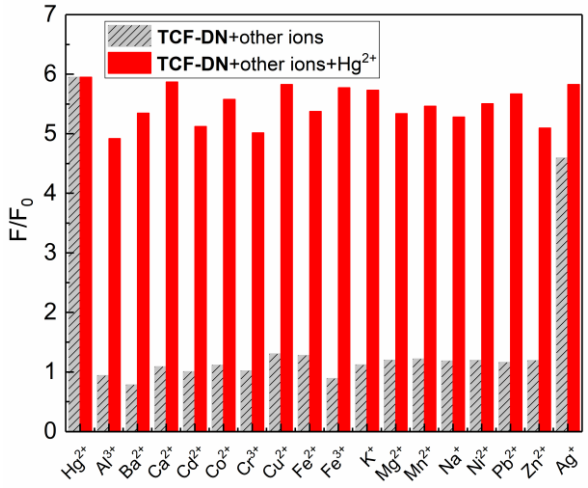


**Figure 5.** Changes in fluorescence intensity ratios ($F/F_0$) of probe **1** (10 μM) upon addition of different metal ions (30 μM) and followed by further addition of $Hg^{2+}$ (30 μM). $\lambda_{em}$ = 625 nm

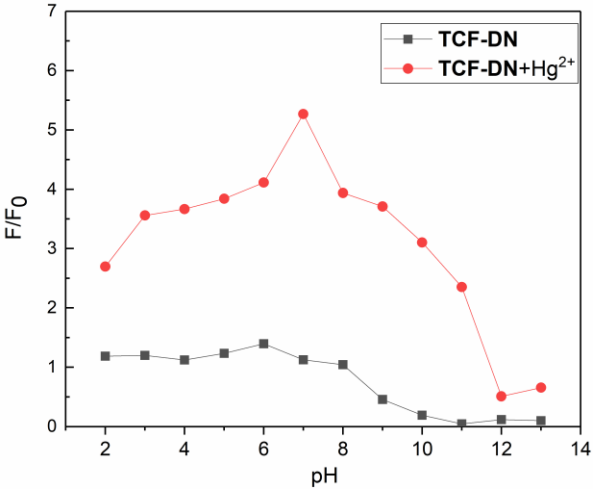


**Figure 6.** Fluorescence intensity ratios ($F/F_0$) changes of probe **1** in the presence and absence of $Hg^{2+}$ at different pH conditions

**Detection mechanism of probe 1 to $Hg^{2+}$**

The sensing mechanism of probe **1** for $Hg^{2+}$ may owe to the strong thiophilic characteristic of $Hg^{2+}$, which results in releasing of compound **2** *via* the reaction of probe **1** with $Hg^{2+}$. To confirm this speculation, the HRMS spectrum of the reaction mixture of probe **1**+$Hg^{2+}$ was checked. The peaks appeared at *m/z* = 370.1201 and *m/z* = 352.1094 (Figure S3) can be assigned to the species of [**2**+$H_2O$-H]$^-$ (calcd. *m/z* = 370.1197 [**2**-H]$^-$ (calcd. *m/z* = 352.1092), respectively, which advocating the formation of compound **2** on addition of $Hg^{2+}$ to probe **1** solution. We then separately conducted the reaction of probe **1** with $Hg^{2+}$, and the main product was isolated. The $^1$H NMR spectra of the isolated product were then compared with those of probe **1** and compound **2** (Figure 7). Obviously, the $^1$H NMR spectrum of the isolated product of probe **1**+$Hg^{2+}$ (Figure 7b) is almost identical with that of compound **2** (Figure 7c), proving that reaction of probe with $Hg^{2+}$ indeed gives compound **2**. Based on these processes, the detection mechanism of probe **1** to $Hg^{2+}$ can be explained in Scheme 2.

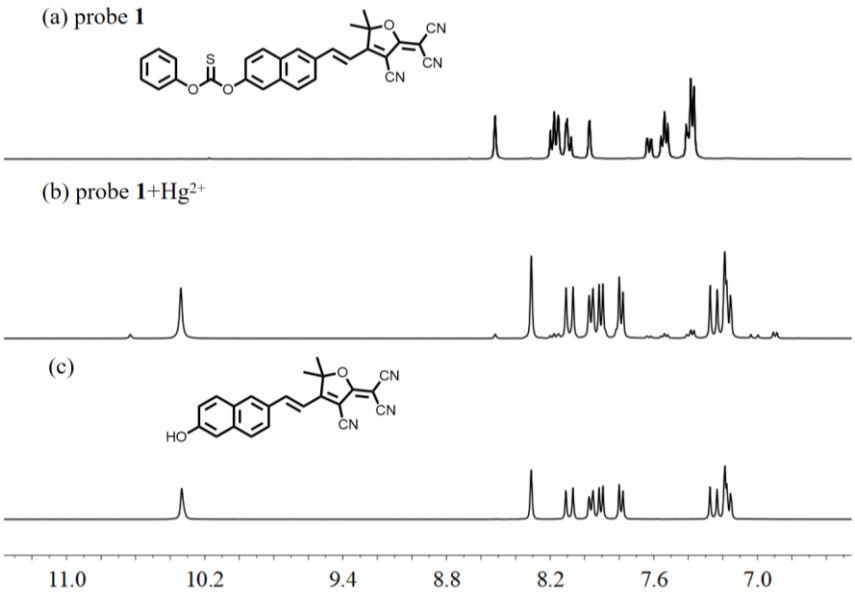


**Figure 7.** Comparison of the $^1$H NMR spectra of probe **1** (a), probe **1**+$Hg^{2+}$ (b) and compound **2** (c) in DMSO-$d_6$

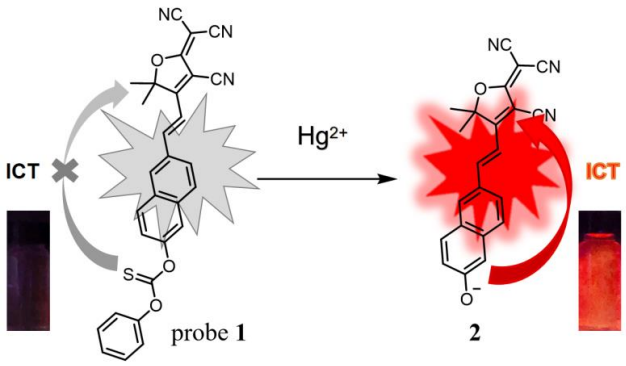


**Scheme 2.** The sensing mechanism of probe **1** to $Hg^{2+}$

**$Hg^{2+}$ imaging in live cells**

Due to the good sensing performance of probe **1** to $Hg^{2+}$, we then explored its application to image $Hg^{2+}$ in living cells. The cell toxicity experiments reveal that probe **1** has low toxicity to MCF-7 cells (Figure S4). Then, live cell imaging experiments were performed on MCF-7 cells. Firstly, MCF-7 cells were incubated with probe **1** (10 μM) for 30 minutes at 37 °C, no fluorescence emission was observed in the red channel (Figure 8b). Then the MCF-7 cells pretreated with the probe were washed 3 times with PBS buffer, after further incubation with different concentrations of $HgCl_2$ (10, 50, and 100 μM) for 30 minutes, obvious red fluorescence can be observed, and the fluorescence brightness increases with the increase of $Hg^{2+}$ concentration (Figure 8b–k). These results indicate that probe **1** has good cell permeability and can image $Hg^{2+}$ in MCF-7 cells.

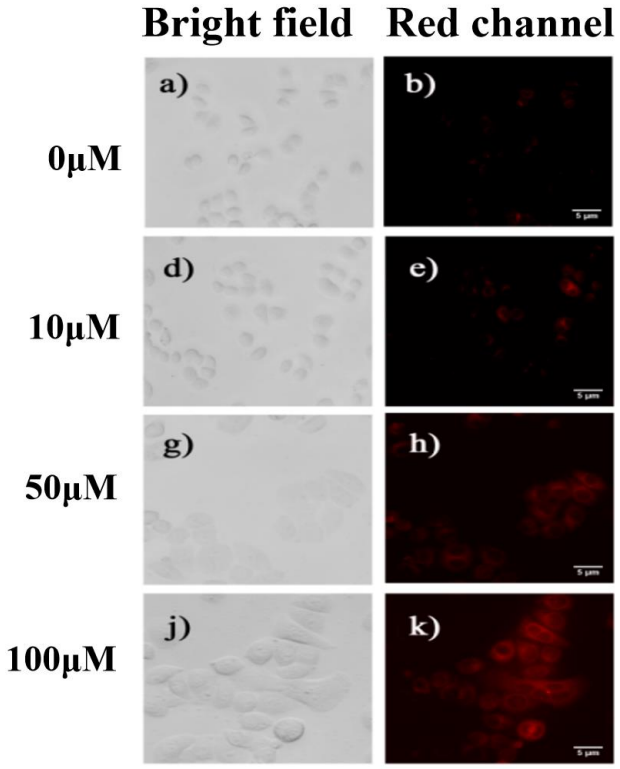


**Figure 8.** Bioimaging of MCF-7 cells incubated with probe **1** (10 μM) and 0 μM, 10 μM, 50 μM and 100 μM $Hg^{2+}$ ions respectively. Left column: Bright field. Right column: Red channel.

In conclusion, we have developed a new TCF-based fluorescent probe **1** for $Hg^{2+}$ recognition in MeOH/Tris (1:1, v/v, Tris 20 mM，pH = 7.4) solution with long-wavelength emission and a large Stokes shift (160 nm). Probe **1** displays rapid response to $Hg^{2+}$ (< 3 min) with a low detection limit (1.06 nM). The recognition mechanism is proved to undergo $Hg^{2+}$-triggered releasing of the precursor compound **2**. Probe **1** has membrane permeability, and is applicable for fluorescence image of $Hg^{2+}$ in living MCF-7 cells.

## ACKNOWLEDGEMENTS

The project was supported by the National Natural Science Foundation of China (Nos. 21878023, U1608222), the Program for Distinguished Professor of Liaoning Province.

## SUPPORTING INFORMATION

Supplementary data (Experimental procedures and details, Characterization data for products, NMR spectra for all products) associated with this article can be found, in the online version, at URL: https://www.heterocycles.jp/newlibrary/downloads/PDFsi/27267/102/10.

## REFERENCES

1. H. Lv, G. Yuan, G, Zhang, Z. Ren, H. He, Q. Sun, X. Zhang, and S. Wang, *Dyes Pigm.*, 2020, **172**, 107658.
2. G. Zhang, A. Ding, Y. Zhang, L. Yang, L. Kong, X. Zhang, X. Tao, Y. Tian, and J. Yang, *Sens. Actuators, B*, 2014, **202**, 209.
3. Y. Wang, G. Zhang, F. Zhang, T. Chu, and Y. Yang, *Sens. Actuators, B*, 2017, **251**, 667.
4. D. Dai, Z. Li, J. Yang, C. Wang, J. R. Wu, Y. Wang, D. Zhang, and W. Yang, *J. Am. Chem. Soc.*, 2019, **141**, 4756.
5. Y. Hou, M. Yan, Q. Wang, Y. Wang, Y. Xu, Y. Wang, H. Li, and H. Wang, *Food Anal. Methods*, 2016, **10**, 1931.
6. Y. Ding, Y. Pan, and Y. Han, *Ind. Eng. Chem. Res.*, 2019, **58**, 7786.
7. L. Tang, L. Zhou, X. Yan, K. Zhong, X. Gao, and J. Li, *J. Photochem. Photobiol. A*, 2020, **387**, 112160.
8. C. Zhang, H. Zhang, M. Li, Y. Zhou, G. Zhang, L. Shi, Q. Yao, S. Shuang, and C. Dong, *Talanta*, 2019, **197**, 218.
9. T. Gao, X. Huang, S. Huang, J. Dong, K. Yuan, X. Feng, T. Liu, K. Yu, and W. Zeng, *J. Agric. Food Chem.*, 2019, **67**, 2377.
10. D. Zhang, M. Li, Y. Jiang, C. Wang, Z. Wang, Y. Ye, and Y. Zhao, *Dyes Pigm.*, 2013, **99**, 607.
11. Y. Jiang, Q. Duan, G. Zheng, L. Yang, J. Zhang, Y. Wang, H. Zhang, J. He, H. Sun, and D. Ho, *Analyst*, 2019, **144**, 1353.
12. Y. Zhao, X. Xing, R. Gao, M. Tao, and W. Zhang, *J. Mater. Sci.*, 2018, **53**, 10523.
13. D. Zhang, X. Huang, P. Ding, Z. Wang, Y. Zhao, and Y. Ye, *Sens. Actuators, B*, 2014, **198**, 33.
14. D. Zhang, M. Li, M. Wang, J. Wang, X. Yang, Y. Ye, and Y. Zhao, *Sens. Actuators, B*, 2013, **177**, 997.
15. D. Jiang, J. Zhao, Q. Li, C. L. Sun, J. G. T. Guan, L. and J. Xiao, *Dyes Pigm.*, 2016, **125**, 136.

16. F. H. Wang, C. W. Cheng, L. C. Duan, W. Lei, M. Z. Xia, and F. Y. Wang, *Sens. Actuators, B*, 2015, **206**, 679.
17. L. Tang, J. Xia, K. Zhong, and Y. Tang, *Dyes Pigm.*, 2020, **178**, 108379.
18. S. Erdemir, O. Kocyigit, and S. Malkondu, *J. Photochem. Photobiol. A*, 2015, **309**, 15.
19. L. Tang, L. Zhou, A. Liu, X. Yan, and J. Li, *Dyes Pigm.*, 2021, **186**, 109034.
20. Y. Fang, Y. Zhou, J-Y. Li, Q-Q. Rui, and C. Yao, *Sens. Actuators, B*, 2015, **215**, 350.
21. G. Chen, Z. Guo, G. Zeng, and L. Tang, *Analyst*, 2015, **140**, 540043.
22. W. Luo, H. Jiang, K. Zhang, L. Wei, and W. Liu, *J. Mater. Chem. B*, 2015, **3**, 3459.
23. T. Chatterjee, S. Areti, and M. Ravikanth, *Inorg. Chem.*, 2015, **54**, 2885.
24. X. Ma, Y. Wang, T. Wei, L. Qi, X. Jiang, J. Ding, W. Zhu, H. Yao, Y. Zhang, and Q. Lin, *Dyes Pigm.*, 2019, **164**, 279.
25. B. Khan, A. Hameed, A. Minhaz, and M. R. Shah, *J. Hazard. Mater.*, 2018, **347**, 349.
26. Z. Cheng, G. Li, and M. Liu, *J. Hazard. Mater.*, 2015, **287**, 402.
27. A. Kumar and P. Chae, *Sens. Actuators, B*, 2019, **281**, 933.
28. I. Chang, K. Hwang, and S. Chang, *Dyes Pigm.*, 2017, **137**, 69.
29. M. Choi, H. Ryu, M. Han, and S. Chang, *Tetrahedron Lett.*, 2016, **57**, 4360.
30. S. Q. Zang, W. M. He, Z. Zhou, Z. Han, S. Li, and Z. Zhou, *Angew. Chem. Int. Ed.*, 2021, **133**, 8586.
31. P. Liu, B. Li, J. Zheng, Q. Liang, C. Wu, L. Huang, P. Zhang, Y. Jia, and S. Wang, *Sens. Actuators, B*, 2021, **329**, 129147.
32. Y. Huo, S. Wang, T. Lu, C. Pan, Lu, Y. Yang, X. Hu, and D. S. Hu, *RSC Adv.*, 2016, **6**, 5503.
33. P. Zhou, S. Wu, M. Hegazy, H. Li, X. Xu, H. Lu, and X. Huang, *Mater. Sci. Eng: C*, 2019, **104**, 109914.
34. L. Tang, Y. Sun, K. Zhong, and L. Jin, *Tetrahedron Lett.*, 2020, **61**, 152470.